# Reaction Rate Enhancement for $Cu(In,Ga)Se_2$ Absorber Materials using Ag-alloying

Sina Soltanmohammad[1, 2], Ho Ming Tong[3], Timothy J. Anderson[3], William N. Shafarman[1, 2]

[1]Department of Materials Science & Engineering, 201 Du Pont Hall, University of Delaware, Newark, Delaware 19716, USA
[2]Institute of Energy Conversion, University of Delaware, 451 Wyoming Rd, Newark, Delaware 19716, USA
[3] Chemical Engineering Department, University of Florida, Gainesville, Florida, 32611, USA

***Abstract* — The addition of Ag to Cu-Ga-In precursors for synthesizing $(Ag,Cu)(In,Ga)Se_2$ (ACIGS) thin films has shown benefits including improved adhesion, greater process tolerance and potential for improved device performance. In this study, reaction pathways to form $Cu(In,Ga)Se_2$ (CIGS) and ACIGS were studied by time-progressive reactions at 450°C in a 5% Ar/$H_2Se$ atmosphere followed by *ex-situ* characterization. Results indicated that the addition of 25% Ag/(Ag+Cu) to the CIGS film reduces the reaction time by 50%. X-ray diffraction (XRD) analysis of CIGS films showed that the $CuInSe_2$ phase initially formed after 3.5 min. The slow reaction of the stable $\gamma$-$Cu_9(In,Ga)_4$ phase, however, required more than 20 min to complete the reaction. Importantly, the addition of Ag to the CIGS film accelerated the reaction. Energy-dispersive X-ray spectroscopy show that Ga/(Ga+In) grading occurs in the first 10 min of the reaction. XRD analysis showed that the chalcopyrite phase fully forms after 10 min and no significant changes were observed in samples selenized from 10-45 min. Reaction pathways of Ag-alloyed films were further characterized using *in-situ* high temperature XRD analysis. The onset temperature of Se reaction was detected at 230°C and a $AgIn_2$ phase transformation to $(Ag,Cu)In_2$ occurred in the early stage of the reaction.**

***Index Terms* — $(Ag,Cu)(In,Ga)Se_2$, selenization, reaction pathway, photovoltaic materials.**

## I. Introduction

Silver alloying of $Cu(In,Ga)Se_2$ (CIGS) to $(Ag,Cu)(In,Ga)Se_2$ (ACIGS) has been investigated due to lowering the melting temperature and widening the bandgap of Ag-CIGS alloys [1]. Co-evaporated ACIGS films have shown reduced defect densities [1], increased grain size [2], [3] and enhanced device performance [4], [5] to 19.9% efficiency compared to CIGS deposited with a comparable three-stage co-evaporation process [6].

The formation of ACIGS films by the reaction of Ag-Cu-Ga-In precursors in $H_2Se/H_2S$ has also been reported [7]–[10]. A 10 or 32 nm thick Ag layer in the precursor gave significant improvement in film adhesion that enabled higher reaction temperature and improved device performance [7].

Knowledge of the growth process during the absorber formation is essential to develop a high quality absorber material and therefore high performance solar cells as well as to provide critical input for potential process scale-up. Reaction and phase change chemistry of the formation of ternary and quaternary chalcopyrites from metal precursors has been studied by different groups using time-progressive reactions with *ex-situ* [11]–[13] or *in-situ* analysis [14]–[17]. Verma et al.[11] and Orbey et al.[12] studied the formation of $CuInSe_2$ using time-progressive reactions of Cu-In precursors with $H_2Se$ at 250°C, 325°C and 400°C in a tubular reactor. Brummer et al. [14] and Hergert et al. [15] performed *in-situ* X-ray diffraction analysis during annealing of Se-capped Cu-In bilayer with Se excess in a temperature range from 25 to 550°C. Similar studies also have been done using *in-situ* energy dispersive XRD (EDXRD) [16], [17].

Hergert et al. suggested a two-step process for the formation of the chalcopyrite phase [15]. In the first step, $CuInSe_2$ first forms by reaction of InSe and CuSe at the Se melting temperature (221°C). This is followed by peritectic decomposition of CuSe to $Cu_{2-x}Se$ + Se-rich liquid (276°C), and then fast reaction of InSe and $Cu_{2-x}Se$ to form $CuInSe_2$ as temperature increased. The latter reaction has been verified by other studies while different reactions have been reported for the former steps. This could originate from different processing conditions and precursor designs, uncertainties in the identification of Cu-In phases particularly with rapid *in-situ* XRD scans and possible low temperature phase transformations happening in quenched samples at different stages of the *ex-situ* reaction process [14]. Either of these two analysis has its own challenges. While *ex-situ* analysis suffers from possible low temperature phase transformations during sample quenching, lack of access to the samples during the *in-situ* reactions limits phase identification to XRD data.

Previously, we studied the effect of Ag-alloying on the precursor structure (Cu-In-Ga) using co-sputtered or stacked layer deposition [18] and also reported preliminary results on the reaction pathways using *ex-situ* analysis [19]. Here, we fully determine reaction pathways during the formation of ACIGS using both *ex-situ* and *in-situ* analyses to have a better understanding of the reaction leading to development of an advanced precursor reaction process with a controlled composition profile. Also, the results are compared with the reaction pathways during the formation of CIGS using *ex-situ* analysis. *Ex-situ* analysis using rapid thermal processing (RTP) allows precursors to quickly reach the desired reaction temperature following a rapid quench time.

## II. Experimental Procedures

Ag-Cu-Ga-In metal precursors were deposited onto Mo/soda-lime glass (SLG) substrates by dc magnetron

sputtering at room temperature using $Cu_{0.77}Ga_{0.23}$, $Ag_{0.77}Ga_{0.23}$, and In targets. Samples were deposited with Mo/Cu-Ga/In/Ag-Ga stacked layers, as described previously [9]. Sputtering parameters were determined to give Ag/(Ag+Cu) ≈ 0.25 and (Ag+Cu)/(Ga+In) ≈ 0.90 with an average thickness ≈ 500 nm. Cu-Ga-In metal precursors were sputtered as described in [12]. Selenization was done using rapid thermal processing (RTP) at atmospheric pressure in a tubular quartz reactor. For each run, a precursor was first loaded into the reactor, and then the reactor was charged with 5% $H_2Se$ in Ar similar to a conventional batch reactor. The reaction temperature was 450°C and the reaction time varied from 2 – 45 min. The surface temperature ramp time was set to ~ 1 sec. After reaction, the lamp is turned off and taken away from the sample and Ar is flown into the tube. Cool-down time of the sample surface temperature was ~ 30 sec to 250°C. Temperature is predicted and controlled using a pyrometer and heat transfer models [20].

Sample composition was measured by X-ray fluorescence (XRF) and energy dispersive X-ray spectroscopy (EDS). The XRF measurements sampled the entire film. EDS, however, with excitation voltage 20 keV gives a composition value weighted toward the top 0.3 – 0.5 μm of the film. Cross-section EDS mapping was performed with 10 keV electrons to decrease the interaction volume. The crystal structures of the films were evaluated using symmetric θ-2θ X-ray diffraction (XRD) and glancing incidence XRD (GIXRD) with Cu Kα radiation. XRD patterns were analyzed using the ICDD database [21] and Rietveld refinements were performed by JADE software (Materials Data, Inc. (MDI) JADE 2010). Raman spectra were measured at room temperature with laser illumination at 532 nm. Laser power was set at the lowest available level (0.1 mW) to prevent peak shifting from local heating. The phases and composition variations at the chalcopyrite/Mo interface were studied by delamination of reacted films from Mo/SLG substrate using the techniques described in [13].

*In-situ* high temperature XRD (HTXRD) was used to follow phase evolution during selenization of precursors. The HTXRD instrument consisted of a Panalytical X'Pert Pro diffractometer with a Cu X-ray source paired with an Anton Parr XRK-900 furnace with X-ray transparent Be windows. A detailed description of the system is provided in [22]. Precursors were sealed in a gas tight 304 stainless steel reactor (~6 $cm^3$ inner volume) fitted with X-ray transparent Al windows. Although the reactor was sealed in air, no oxidation of the sample was observable by XRD. *In-situ* analysis started with a high-resolution scan at room temperature and followed by stepping the temperature to 600°C in 10°C steps. An XRD pattern was then acquired in 7-10 min at each step.

## III. Results and Discussion

### A. *Ex-situ analysis*

Cross-sectional SEM images (Fig. 1) of the reacted Ag containing films show morphology evolution during formation of the chalcopyrite phase. Cross-section SEM images of the as-deposited metal precursor show agglomerated nodules due to complex growth of In as previously discussed [9], [18].

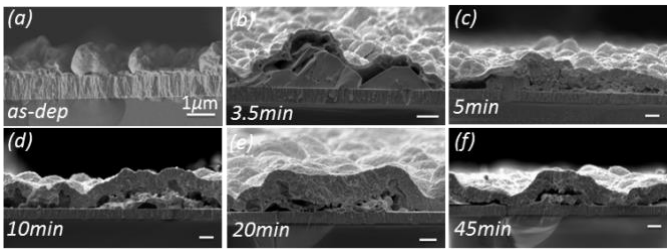


Fig. 1. Cross-sectional SEM images of the (a) as-deposited and reacted films for (b) 3.5 min, (c) 5 min, (d) 10 min, (e) 20 min and (f) 45 min reaction time. Scale bars correspond to 1 μm.

The rougher and less uniform morphology seen in the cross-sectional images Fig 1(d-f) is attributed to slow reaction of stable intermetallic phases such as κ-$(Cu,Ga)_2(Ag,In)$ [23] or $Cu_9(In,\underline{Ga})_4$ [13] (underlines show the most prominent element in the parenthesis), which eventually leave voids at the substrate/film interface after coupled diffusion and reaction. Localized unreacted intermetallic grains separated from a thin selenide top layer are seen in Fig. 1(b). As expected, cross-sectional images show increasing thickness of the selenized layer with reaction time, reaching ~1.5 μm after reacting for 45 min, Fig. 1(c-f).

Fig. 2 shows the Ga/(Ga+In) molar ratio measured by EDS and Se/M ≡ Se/(Ag+Cu+Ga+In) molar ratio measured by both EDS and XRF versus reaction time. Front-side EDS results show Ga grading occurs in the first 10 min. Based on EDS analysis, Se/M reaches ~1.02 after 45 min, however, the bulk Se/M profile measured by XRF analysis indicated a gradual increase to ~0.93 by 10 min. Se uptake is the indicator of the reaction completion with Se/M ≈ 1 indicating that the reaction is completed. The difference between EDS and XRF in Se/M for 5-10 min is consistent with the depth of fully reacted material moving through the film to the back side.

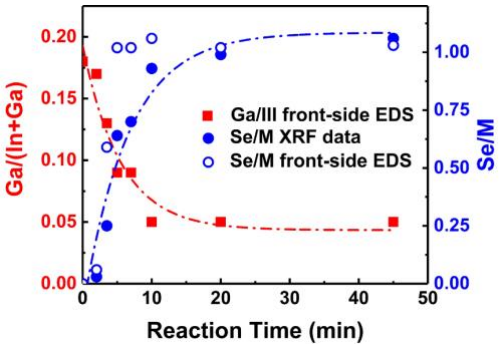


Fig. 2. Ga/(Ga+In) and Se/M profile vs. reaction time measured by EDS and XRF. Lines are a guide to the eye.

Symmetric XRD scans of the as-deposited precursor and reacted films are shown in Fig. 3. These results show that the as-deposited precursor contains $(\underline{Ag},Cu)In_2$ (PDF# 65-1552), In

(PDF# 5-0642), $Cu_3Ga$ (PDF# 44-1117) and $Cu_9(In,Ga)_4$ (PDF# 2-1253) phases. XRD analysis of the films annealed and selenized for 2 min are similar, notably that no crystalline selenide phases are detected (Fig. 4). Raman spectroscopy, however, can provide phase information and is more sensitive to the top surface region. The Raman spectrum shown in Fig. 5(a) shows amorphous In-Se phases on the surface of the film after 2 min reaction. The broad band spreading from the lowest frequency to about 240 $cm^{-1}$ is a common feature of Raman spectra of amorphous In-Se films [24]. Raman modes related to γ-$(In,Ga)_2Se_3$ [24], InSe [25] and $(In,Ga)_4Se_3$ [26] phases are shown in Fig. 5(a). XRD phase analysis of the 2 min annealed or selenized films indicated existence of In, $(Ag,Cu)In_2$, ζ-$Ag_3(In,Ga)$ (PDF#15-163) and $Cu_9(In,Ga)_4$ phases, while peaks at 2θ = 21.6, 35.7, 42.1, and 44.1° (indicated by a star in Fig. 3 and Fig. 4) were matched with the new Laves phase κ-$(Cu,Ga)_2(Ag,In)$ [18], [23]. This phase formed while the as-deposited $Cu_3Ga$ phase dissipated.

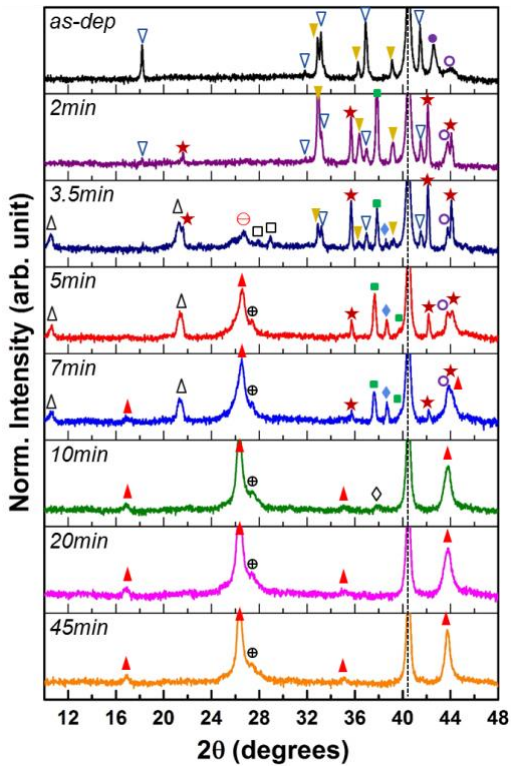


Fig. 3. XRD patterns (square-root scale) of the (a) as-deposited and selenized films at 450°C for 2-45 min reaction time. Phases are indicated as; ◊: In, ?: $(Ag,Cu)In_2$, ●: $Cu_3Ga$, ○: γ-$Cu_9(In,Ga)_4$, ❑: ζ-$Ag_3(In,Ga)$, ★: κ-$(Cu,Ga)_2(Ag,In)$, ♦: γ-$Ag_9(In,Ga)_4$, ❦: α-$(Ag)_{Ga}$, ✕: InSe, ☐: $In_4Se_3$, ⛵: $CuGaSe_2$, ⊖: $CuInSe_2/CuIn_3Se_5$ and 🚌: $(Ag,Cu)(In,Ga)Se_2$. The strong Mo peak is indicated by the dashed line.

After increasing the reaction time to 3.5 min, crystalline InSe (PDF# 01-073-0609) and $In_4Se_3$ (PDF# 01-071-0521) were evident in the XRD analysis (Fig. 3). The broad peak centered at 2θ = 26.7° is attributed to formation of either $CuInSe_2$ (PDF# 40-1487) or the $CuIn_3Se_5$ (PDF# 51-1221) ordered defect compound (ODC) since their diffraction patterns are similar. However, the $CuInSe_2$ phase was not identified in the cross-sectional EDS analysis (Fig. 6), but a Cu-poor chalcogenide phase was detected on the surface. Fig. 5 shows the Raman analysis from the near surface of the reacted films. The spectrum of the 3.5 min reacted sample is similar to that for the 2 min reacted film. However, the overlaps between $A_1$ Raman mode of the $CuInSe_2$ (174-176 $cm^{-1}$[27], [28]) and $CuIn_3Se_5$ (154 $cm^{-1}$[29]) with the In-Se modes rendered phase identification challenging. On the other hand, the XRD intensity of intermetallic phases, particularly In, $(Ag,Cu)In_2$, and ζ-$Ag_3(In,Ga)$ phases were decreased. Also a peak at 2θ = 38.6° appeared and was attributed to γ-$Ag_9(In,Ga)_4$ (PDF# 31-564). Interestingly, Fig. 6 also shows the formation of the κ-$(Cu,Ga)_2(Ag,In)$ intermetallic phase under a thin selenide layer.

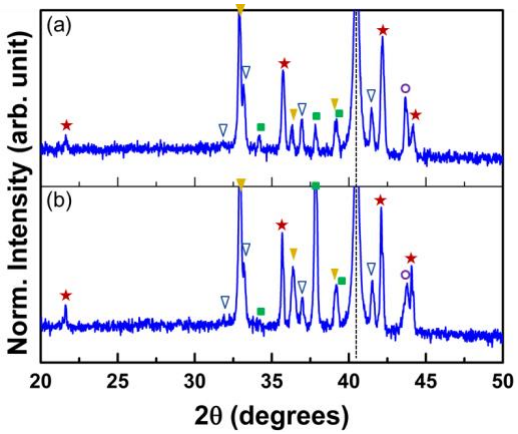


Fig. 4. XRD patterns (square-root scale) of the (a) Ar annealed and selenized films at 450°C for 2 min. Phases are indicated as; ◊: In, ?: $(Ag,Cu)In_2$, ○: γ-$Cu_9(In,Ga)_4$, ❑: ζ-$Ag_3(In,Ga)$ and ★: κ-$(Cu,Ga)_2(Ag,In)$. The Mo peak is indicated by the dashed line.

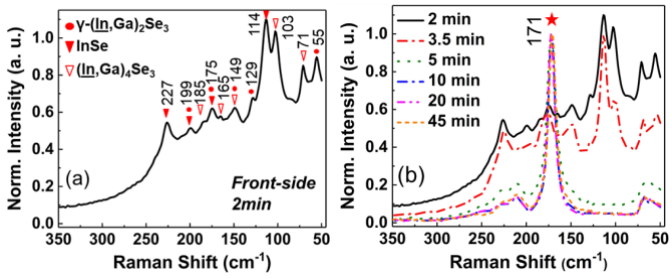


Fig. 5. (a) Raman scattering spectra from the near surface region of the film reacted at 450°C for 2 min showing formation of amorphous In-Se phases on the surface. (b) Raman spectra of films reacted for 2-45 min. Raman modes were indicated as; ●: γ-$(In,Ga)_2Se$, ◊: InSe and ?: $(In,Ga)_4Se_3$, ★: chalcopyrite $A_1$ mode. Raman modes of reacted films for 2 and 3.5 min were similar so not duplicated in figure (b).

The Raman scattering spectrum from the near surface region of the film reacted for 5 min is consistent with formation of the chalcopyrite phase (Fig. 5(b)). The position of the (112)

reflection also shifted to lower 2θ, Fig. 7(a), while its intensity increased. This is accompanied by the disappearance of In and (Ag,Cu)$In_2$ phases and decreasing intensity of the κ-(Cu,Ga)$_2$(Ag,In) phase, while the intensity of the γ-$Ag_9$(In,Ga)$_4$ phase increased (Fig. 3 and Fig. 7(b)). The XRD (002) peak of ζ-$Ag_3$(In,Ga) (at 2θ = 37.84°) also shifted to lower 2θ (Fig. 7(b)). Fig. 8(a) compares the refined lattice constants of ζ-$Ag_3$(In,Ga) phase over the reaction time. It is seen that the 2 and 3.5 min reacted films have similar lattice constants. Increasing the reaction time to 5 and 7 min, however, results in a decrease in the value of *a* and increase in *c*. This is in good agreement with measured lattice parameter values for ζ-$Ag_3$In versus Ag at.% [30], Fig. 8(b). As a result, it is possible that by increasing the reaction time, In reacted to form InSe and chalcogenide phase while the ζ-$Ag_3$(In,Ga) phase was depleted. On the other hand, substitution of Ag/In with smaller Cu/Ga or residual stress in the film may have caused the shift.

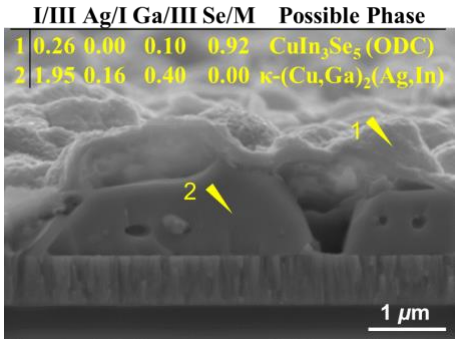


Fig. 6. SEM cross-section and spot-EDS analysis of the 3.5 min reacted film.

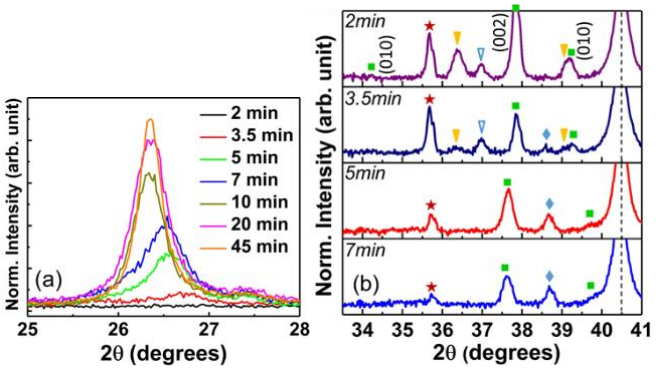


Fig. 7. (a) XRD (112) peak (linear-scale) of the chalcogenide phase and (b) XRD peak positions of ζ-(Ag,Cu)$_3$(In,Ga) over reaction time. Phases are indicated as; ◊: In, ?: (Ag,Cu)$In_2$, □: ζ-$Ag_3$(In,Ga), ♦: γ-$Ag_9$(In,Ga)$_4$, and ★: κ-(Cu,Ga)$_2$(Ag,In). The Mo peak is indicated by the dashed line.

The XRD pattern of the 7 min reacted film is similar to that of the one reacted for 5 min, (Fig. 3). The intensity of the chalcogenide phase, however, increased (Fig. 7(a)). The results of SEM/EDS cross-sectional analysis of the 7 min reacted film (Fig. 9) show localized intermetallic compounds that are fully separated from the top chalcogenide layer. EDS mapping further shows two different grains with compositions corresponding with γ-$Cu_9$(In,Ga)$_4$ and κ-(Cu,Ga)$_2$(Ag,In).

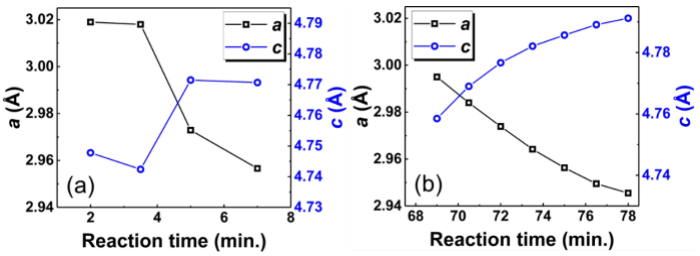


Fig. 8. (a) Refined lattice constants of ζ-$Ag_3$(In,Ga) versus reaction time, and (b) ζ-$Ag_3$In lattice constant measured by King et al.[30].

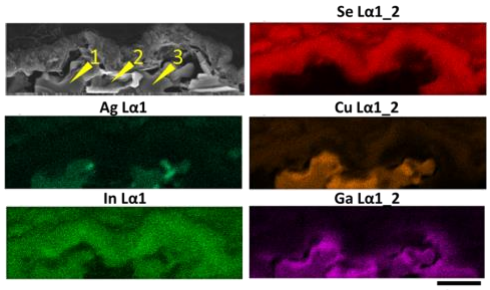


| Spot | (Ag+Cu)/ (In+Ga) | Ag/ (Ag+Cu) | Ga/ (In+Ga) | Se/ Metal | Possible Phase |
|---|---|---|---|---|---|
| 1 | 2.0 | 0.2 | 0.4 | 0.0 | κ-(Cu,Ga)$_2$(Ag,In) |
| 2 | 2.0 | 0.0 | 0.9 | 0.0 | γ-$Cu_9$(In,Ga)$_4$ |
| 3 | 1.9 | 0.2 | 0.4 | 0.0 | κ-(Cu,Ga)$_2$(Ag,In) |

Fig. 9. Cross-sectional SEM/EDS elemental maps of the sample selenized for 7 min. EDS point analysis also is shown in the table.

XRD analysis of the sample selenized for 10 min (Fig. 3) shows almost no sign of intermetallic phase formation. The cross-sectional EDS analysis in Fig. 10, however, reveals the existence of localized α-(Ag) and $Cu_9Ga_4$ residues at the back interface. The XRD (112) peak of the chalcogenide phase is shifted to lower 2θ (Fig. 7(a)), consistent with incorporation of larger Ag atoms onto the group 1 sub-lattice. No significant changes are seen in the XRD patterns of samples selenized for 10 to 45 min, indicating that the chalcogenide phase fully formed after ~10 min reaction. Lattice constants estimated from Rietveld analysis ($a = 5.83$ Å, $c = 11.73$ Å) are consistent with those reported for the ($Ag_{0.25}Cu_{0.75}$)$InSe_2$ phase [31]. The shoulder peak on the right side of the (112) peak of (Ag,Cu)$InSe_2$ phase (Fig. 3) is possibly related to formation of a high Ga content chalcopyrite phase. To verify this hypothesis, reacted films were peeled from the substrate and remnants on the Mo side were analyzed using SEM/EDS and Raman spectroscopy. Fig. 11 shows the Raman spectrum of a remnant on the Mo side of the film selenized at 450°C for 45 min. The intense Raman peak at 182 $cm^{-1}$ is in good agreement with the reported values for the $A_1$ Raman mode of the $CuGaSe_2$ (CGS) phase [27], [32]. Other CGS Raman modes were identified at around 57, 94, 117, 240 and 269 $cm^{-1}$.

$CuGa_3Se_5/CuGa_5Se_8$ ODC layers were also identified with Raman. The peak near 160 $cm^{-1}$ can be assigned to the A1 mode, the peaks near 250/285 $cm^{-1}$ can be assigned to B2/E modes [32], [33]. Vacancies in the ODC phases relax the stretching-forces, therefore reducing the corresponding vibrational frequencies for the normal chalcopyrite (CGS) [29]. A high concentration of the defects in these phases also causes broadening of the Raman peaks [32]. Additional Raman studies (not shown here) also indicated formation of GaSe remnants at the backside of the film and $MoSe_2$ on the Mo side.

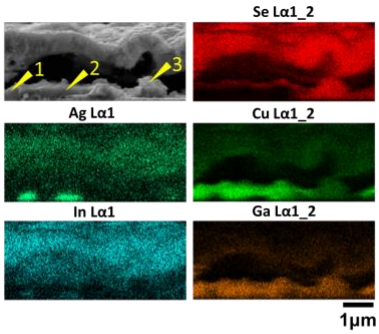


| Spot | (Ag+Cu)/ (In+Ga) | Ag/ (Ag+Cu) | Ga/ (In+Ga) | Se/ Metal | Possible Phase |
|---|---|---|---|---|---|
| 1 | 1.9 | 0.0 | 1.0 | 0.0 | γ-$Cu_9Ga_4$ |
| 2 | 2.6 | 0.4 | 1.0 | 0.0 | γ-$Cu_9Ga_4$ / (Ag) |
| 3 | 1.0 | 0.0 | 1.0 | 1.0 | $CuGaSe_2$ |

Fig. 10. Cross-sectional SEM and EDS mapping of the sample selenized for 10 min reaction. EDS point analysis also is shown in the table.

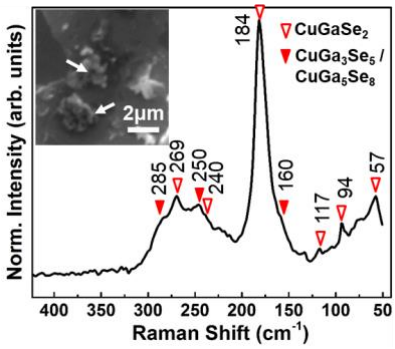


Fig. 11. Raman scattering spectrum of a remnant on the Mo side of the film selenized at 450°C for 45 min. The inset is the SEM image of a remnant at the Mo side of the film.

Based on the data presented, Fig. 12 summarizes the reaction pathway leading to formation of (Ag,Cu)(In,Ga)$Se_2$ absorber layer at 450°C for 45 min reaction time by the *ex-situ* time-progressive experiments.

*B. in-situ HTXRD analysis*

HTXRD *in-situ* measurements reveal phase transformations as a function of both time and temperature while avoiding changes upon cooling. The reaction, however, takes place continuously during ramp/hold and measure stepping sequence. The *ex-situ* characterizations are only a function of time, but also include possible changes during cooling. The comparison of both methods, however, reveals many similar transformations. Fig. 13 displays the HTXRD patterns during the reaction of the metal precursors with Se vapor in the temperature range of 50-600°C. The precursor consisted of similar phases as shown in Fig. 3, except for the presence (Ag,Cu)$In_2$. We have previously shown that this phase formed either by aging the precursor over a week or annealing at temperature below 150°C [18]. Here, aging prior to the analysis led to formation of this phase (Fig.13). At 130°C, the $AgIn_2$ phase transformed to (Ag,Cu)$In_2$. At the same temperature, the intensity of $Cu_3Ga$ and In peaks decreased while the intensity of $Cu_9(In,Ga)_4$ peaks increased, which correspond to phases present in the *ex-situ* samples after reacting for 2 min. Contrary to the *ex-situ* experiments, however, ζ-$Ag_3In$ was not observed during the *in-situ* characterization, indicating that ζ-$Ag_3In$ maybe have formed only during the cooling of *ex-situ* samples. By 220°C, (Ag,Cu)$In_2$ disappeared and the κ-$(Cu,Ga)_2(Ag,In)$ and γ-$Ag_9(In,Ga)_4$ phases formed. The phase transitions are similar to those in the *ex-situ* samples after reacting for 3.5 min.

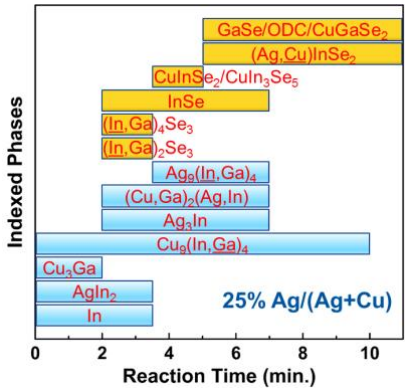


Fig. 12. Summarized reaction pathway for synthesis of ACIGS with Ag/(Ag+Cu) ≈ 25% at 450ºC. Intermetallic and selenide phases were differentiated by blue and yellow colors, respectively.

Formation of the Cu-In-Se/$Cu_{2-x}Se$ phase was initially observed just above the Se melting temperature (221°C) at 230°C. At 320°C, the κ-$(Cu,Ga)_2(Ag,In)$ phase disappeared and the (112) chalcopyrite peak began shifting to lower 2θ values. This peak shift was too large to attribute solely to thermal expansion of the chalcopyrite lattice. Incorporation of larger Ag atoms into the chalcopyrite lattice, which was observed in the *ex-situ* sample after reacting for 5 min, was therefore hypothesized to contribute to the observed peak shift. At 410°C, the $MoSe_2$ $(10\bar{1}0)$ peak was first detected and accompanied by an expected decrease in the Mo peak intensity. The appearance of $MoSe_2$ is associated with complete reaction of the chalcopyrite at the back interface and consistent with equilibrium predictions [34]. As temperature increased, greater $MoSe_2$ formation was observed when compared to the *ex-situ*

process. This may be due to the different process conditions. In addition, it's been shown that background pressure (not just initial Se loading) has a large effect on the thickness of the $MoSe_2$ [35]. The expected overall pressure of *in-situ* reactor at 600°C is close to 3.2 atm [35]. HTXRD isoline patterns shown in Fig. 14 display the HTXRD intensity variations during the reaction.

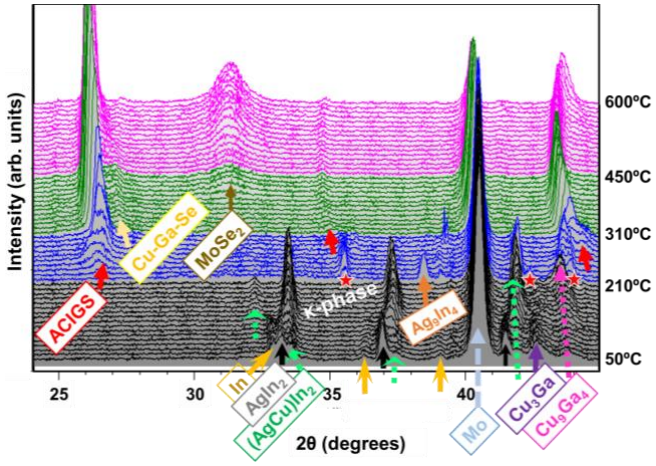


Fig. 13. A serries of HTXRD patterns during formation of the ACIGS absorber layer in the temperature range 50-600°C. Only the prominent element in the compound is shown in the labels on the figure.

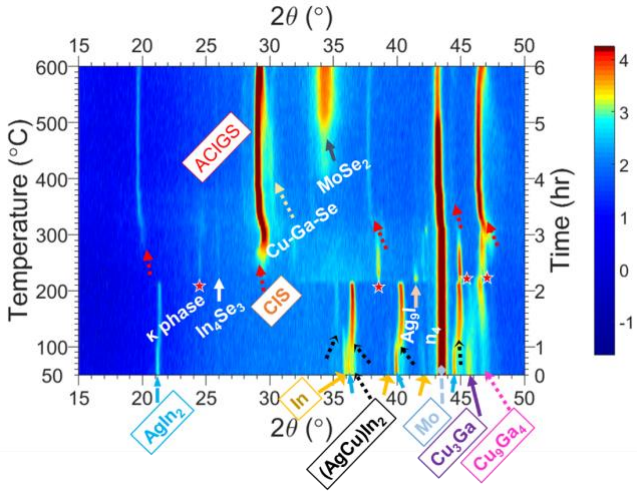


Fig. 14. HTXRD Isoline patterns during formation of the ACIGS absorber layer in the temperature range 50-600°C. Only the prominent element in the compound is shown in the labels on the figure.

### *C. Cu(In,Ga)Se₂*

To compare the reaction analysis before and after Ag-alloying, the reaction pathway to formation of $Cu(In,Ga)Se_2$ was also investigated by *ex-situ* time progressive experiments. XRD analysis of each sample is shown in Fig. 15. As-deposited precursor contains In and $Cu_{16}(\underline{In},Ga)_9$ phases. After 2 min reaction InSe, $(\underline{In},Ga)_4Se_3$ and $\gamma$-$Cu_9(In,\underline{Ga})_4$ phases were identified in the XRD pattern accompanied with In and $Cu_{16}(\underline{In},Ga)_9$ phases. A hump at $2\theta \approx 27^\circ$ can be related either to Cu-Se or $CuInSe_2$ (CIS) phases. With increasing the reaction time to 3.5 min, an intense (112) peak of $CuInSe_2$ phase appeared at $2\theta \approx 26.7^\circ$, while the In and $Cu_{16}(\underline{In},Ga)_9$ intermetallic phases had disappeared. The amount of free In decreases with reaction time, which decreases the In concentration in $\gamma$-$Cu_9(In,\underline{Ga})_4$. This shifts the reflection of the (114) peak ($2\theta \approx 43.3^\circ$) to higher $2\theta$ values and convoluted with the chalcopyrite (220/204) peaks at $2\theta \approx 44.3^\circ$. Between 15 to 20 min reaction time, $\gamma$-$Cu_9(In,\underline{Ga})_4$ reacts to form $CuGaSe_2$ (CGS), which is detected after 20 min just to the right of the $CuInSe_2$ (112) peak. On the other hand, InSe is evident in the XRD patterns to 15 min. With formation of CGS at 20 min, InSe disappeared and only chalcogenide phases were detected. There was no significant change in the XRD patterns between 20-45 min except peak sharpening after 45 min, consistent with crystallinity improvement of the chalcogenide phases. There is a broad peak on the low $2\theta$ side of the $CuInSe_2$ (112) peak in films reacted for 3.5-20 min that can be attributed to formation of a $Cu_{2-x}Se$ phase with orthorhombic crystal structure.

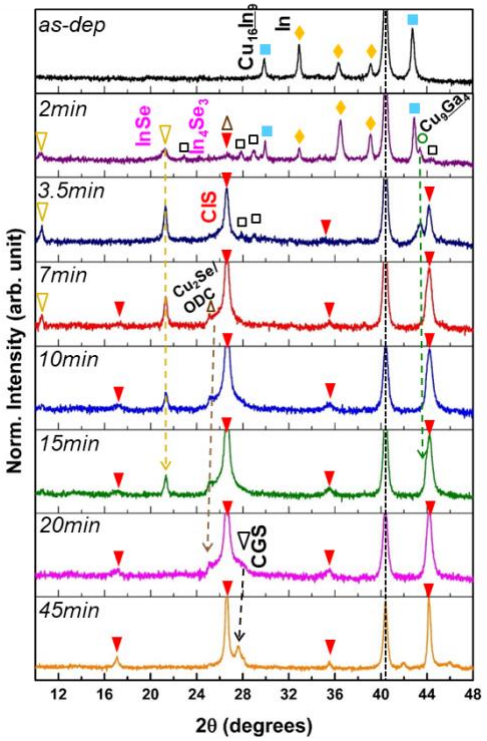


Fig. 15. XRD patterns of as-deposited and reacted Ag/(Ag+Cu) = 0.0 films for different reaction times. Phases are indicated as; ■: In, ○: $\gamma$-$Cu_9(In,\underline{Ga})_4$, □: $Cu_{16}(In,Ga)_9$, ✕: $Cu_{2-x}Se$ / Cu-In-Se (ODC), ❓; InSe, ☐: $In_4Se_3$,: ❓: $Cu(In,\underline{Ga})Se_2$, and ↻: $Cu(\underline{In},Ga)Se_2$. The strong Mo peak is indicated by the dashed line.

Raman scattering analysis indicated formation of $Cu_{2-x}Se$ on the surface of the film reacted for 10-20 min (not shown here). This phase was formed between 3-7 min reaction and vanished at 45 min. Based on XRD analysis, the other possible phase is

$Cu_3In_5Se_9$ or the so-called "ordered defect compound, (ODC)". It also has orthorhombic crystal structure with *Pmm*2 space group. Fig. 16 shows the Se and Ga profiles of the Ag/(Ag+Cu) = 0.0 films versus reaction time. Based on EDS analysis, Se reaches its stoichiometric composition within the top 0.5 µm of the film after 3.5 min reaction; while the entire Se/M profile measured by XRF indicated 0.49 for the same sample. XRF data indicated a gradual increase in Se/M to 0.80 after 20 min reaction.

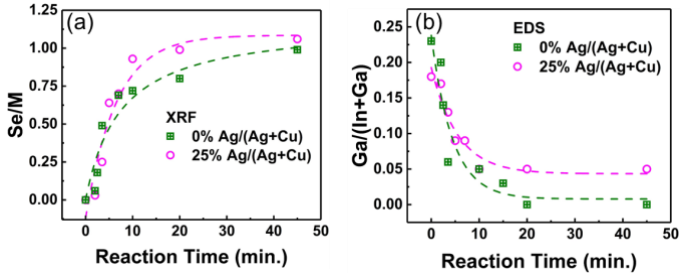


Fig. 16. Comparing Se/Metals (a) and Ga/(Ga+In) (b) profiles versus reaction time measured for as-deposited and reacted Ag/(Ag+Cu) ≈ 0.0 and 0.25 films. Se uptake was measured by EDS and XRF while Ga grading was measured with EDS.

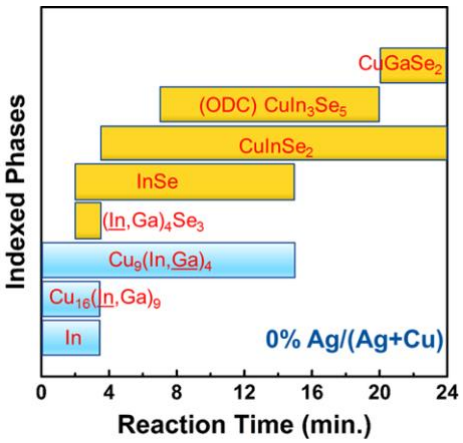


Fig. 17. Reaction pathway analysis of formation of chalcopyrite phase with Ag/(Ag+Cu) = 0.0 at 450°C. Intermetallic and selenide phases were differentiated by blue and yellow colors, respectively.

EDS indicated that the Ga concentration near the surface of the films was gradually lowered by increasing the reaction time and was eventually full depleted at the surface after 20 min of reaction. These results together with XRD data indicate that the $CuInSe_2$ phase was initially formed on the surface of the film after 3.5 min, while the Ga remained in the stable γ-$Cu_9(In,Ga)_4$ phase. Then it reacts into $CuGaSe_2$ phase at the back of the sample between ~15-25 min reaction time. Fig. 16 also compares the Se and Ga profiles of the Ag/(Ag+Cu) = 0.0 and 0.25 films versus reaction time. It indicates that Se uptake occurs about two times faster in films with Ag/(Ag+Cu) = 0.25 than those with no Ag. Also, the Ga graded towards the back interface in all films. Measurement on films with Ag/(Ag+Cu) = 0.25, however, showed slightly higher Ga in top 0.3 – 0.5 µm of the film, which is attributed to the lower melting temperature of alloys with higher Ag content. Fig. 17 summarizes the reaction pathways leading to formation of the $Cu(In,Ga)Se_2$ absorber at 450°C for 45 min reaction time by the *ex-situ* time-progressive experiments.

## IV. Conclusions

In this study, the reaction pathway for synthesis of $(Ag,Cu)(In,Ga)Se_2$ thin films by selenization of metal precursor films was studied using both *ex-situ* and *in-situ* characterization. XRD analysis of *ex-situ* reacted films with Ag/(Ag+Cu) = 0.0 indicated that the $CuInSe_2$ phase initially formed after 3.5 min. However, due to slow reaction of a stable γ-$Cu_9(In,Ga)_4$ phase the complete reaction required more than 20 min. Importantly, the addition of Ag into the CIGS film accelerated the reaction. EDS/XRF results showed that the Se uptake occurred in the first 10 min of the reaction at 450°C. This indicated that the addition of 25% Ag/(Ag+Cu) to the CIGS film reduces the reaction time by 50%. XRD analysis of Ag alloyed samples annealed/selenized at 450°C for 2 min was similar, although Raman spectroscopy indicated the formation of amorphous In-Se phases. The chalcopyrite crystalline peak was first observed after 3.5 min reaction time and its intensity increased up to 10 min reaction, and no significant changes subsequently observed. SEM/EDS and Raman studies on the back side of the films indicated formation of $CuGa_3Se_5$/$CuGa_5Se_8$, GaSe and $CuGaSe_2$ and phases at the back interface of the films. *In-situ* HTXRD analysis of the Ag/(Ag+Cu) ≈ 0.25 films also verified the reaction pathways. The onset temperature of Se reaction was detected at 230°C, which just above the Se melting temperature. HTXRD analysis indicated a $AgIn_2$ phase transformation into $(Ag,Cu)In_2$ in the early stage of the reaction. Most of the intermetallic phases disappeared at T ≈ 320°C, while the (112) chalcopyrite peak started to shift to lower 2θ at higher temperature suggesting mixing between chalcopyrite regions but with different compositions on either the group I or III sub-lattices.

## Acknowledgements

The authors acknowledge the technical support of John Elliott, Kevin Hart and Wayne Buchanan. This material is based, in part, upon work supported by the U.S. Department of Energy's Office of Energy Efficiency and Renewable Energy (EERE) under Solar Energy Technologies Office (SETO) Agreement Number DE-EE0005407. HTXRD was conducted though the Center for Nanophase Materials Sciences user program (project number: CNMS2014-366) at the Oak Ridge National Laboratory with support from Jong K. Keum and Adam Rondinone. This material is based, in part, upon work supported by the Department of Energy under Award Number DE-EE0005407. HTXRD was conducted though the Center for Nanophase Materials

Sciences user program (project number: CNMS2014-366) at the Oak Ridge National Laboratory.

## REFERENCES


[1] P. Erslev, G. M. Hanket, W. N. Shafarman, and D. J. Cohen, "Characterizing the effects of silver alloying in chalcopyrite CIGS with junction capacitance methods," in *MRS Proceedings*, 2011, vol. 1165, pp. 1165-M01-7.

[2] L. Chen, J. Lee, B. E. McCandless, S. Soltanmohammad, and W. N. Shafarman, "Characterization of group I-rich growth during (Ag,Cu)(In,Ga)$Se_2$ three-stage co-evaporation," in *2014 IEEE 40th Photovoltaic Specialist Conference (PVSC)*, 2014, pp. 0332–0336.

[3] L. Chen, S. Soltanmohammad, J. Lee, B. E. McCandless, and W. N. Shafarman, "Secondary phase formation in (Ag,Cu)(In,Ga)$Se_2$ thin films grown by three-stage co-evaporation," *Sol. Energy Mater. Sol. Cells*, vol. 166, pp. 18–26, 2017.

[4] W. Shafarman, C. Thompson, J. Boyle, G. Hanket, P. Erslev, and J. David Cohen, "Device characterization of (AgCu)(InGa)$Se_2$ solar cells," in *2010 35th IEEE Photovoltaic Specialists Conference*, 2010, pp. 000325–000329.

[5] M. Edoff *et al.*, "High Voc in (Cu,Ag)(In,Ga)$Se_2$ solar cells," in *2017 IEEE 44th Photovoltaic Specialists Conference (PVSC)*, 2017.

[6] C. P. Thompson, L. Chen, W. N. Shafarman, J. Lee, S. Fields, and R. W. Birkmire, "Bandgap gradients in (Ag,Cu)(In,Ga)$Se_2$ thin film solar cells deposited by three-stage co-evaporation," in *2015 IEEE 42nd Photovoltaic Specialist Conference (PVSC)*, 2015, pp. 1–6.

[7] Y. Tauchi, K. Kim, H. Park, and W. Shafarman, "Characterization of (AgCu)(InGa)$Se_2$ absorber layer fabricated by a selenization process from metal precursor," *IEEE J. Photovoltaics*, vol. 3, no. 1, pp. 467–471, 2013.

[8] S. Soltanmohammad, L. Chen, B. E. McCandless, and W. N. Shafarman, "Phase stability in Ag-Cu-In-Ga metal precursors for (Ag,Cu)(In,Ga)$Se_2$ thin films," *Sol. Energy Mater. Sol. Cells*, vol. 172, 2017.

[9] S. Soltanmohammad, D. M. Berg, L. Chen, K. Kim, H. Simchi, and W. N. Shafarman, "Effect of sputtering sequence on the properties of Ag-Cu-In-Ga metal precursors and reacted (Ag,Cu)(In,Ga)$Se_2$ films," in *2014 IEEE 40th Photovoltaic Specialist Conference (PVSC)*, 2014, pp. 1707–1711.

[10] S. Soltanmohammad and W. N. Shafarman, "Reaction pathway analysis of $(Ag_xCu_{1-x})(In_{0.75}Ga_{0.25})Se_2$ with x = 0.75 and 1.0," *Sol. Energy Mater. Sol. Cells*, vol. 182, 2018.

[11] S. Verma and N. Orbey, "Chemical reaction analysis of copper indium selenization," *Prog. Photovoltaics Res. Appl.*, vol. 4, pp. 341–353, 1996.

[12] N. Orbey, H. Hichri, R. Birkmire, and T. Russell, "Effect of temperature on copper indium selenization," *Prog. Photovoltaics Res. Appl.*, vol. 5, pp. 237–247, 1997.

[13] G. M. Hanket, W. N. Shafarman, B. E. McCandless, and R. W. Birkmire, "Incongruent reaction of Cu–(InGa) intermetallic precursors in $H_2Se$ and $H_2S$," *J. Appl. Phys.*, vol. 102, no. 7, p. 74922, 2007.

[14] A. Brummer, V. Honkimäki, P. Berwian, V. Probst, J. Palm, and R. Hock, "Formation of $CuInSe_2$ by the annealing of stacked elemental layers—analysis by in situ high-energy powder diffraction," *Thin Solid Films*, vol. 437, no. 1–2, pp. 297–307, 2003.

[15] F. Hergert, R. Hock, A. Weber, M. Purwins, J. Palm, and V. Probst, "In situ investigation of the formation of Cu(In,Ga)$Se_2$ from selenised metallic precursors by X-ray diffraction—The impact of Gallium, Sodium and Selenium excess," *J. Phys. Chem. Solids*, vol. 66, no. 11, pp. 1903–1907, 2005.

[16] E. Rudigier, J. Djordjevic, C. von Klopmann, B. Barcones, A. Pérez-Rodríguez, and R. Scheer, "Real-time study of phase transformations in Cu–In chalcogenide thin films using in situ Raman spectroscopy and XRD," *J. Phys. Chem. Solids*, vol. 66, no. 11, pp. 1954–1960, 2005.

[17] J. Djordjevic, E. Rudigier, and R. Scheer, "Real-time studies of phase transformations in Cu–In–Se–S thin films—3: Selenization of Cu–In precursors," *J. Cryst. Growth*, vol. 294, no. 2, pp. 218–230, 2006.

[18] S. Soltanmohammad, L. Chen, B. McCandless, and W. N. Shafarman, "Ag–Cu–In–Ga Metal Precursor Thin Films for (Ag,Cu)(In,Ga)$Se_2$ Solar Cells," *IEEE J. Photovoltaics*, vol. 7, no. 1, pp. 273–280, 2017.

[19] S. Soltanmohammad and W. N. Shafarman, "Reaction pathway analysis of Ag-alloyed Cu(In, Ga)$Se_2$ absorber materials," in *2016 IEEE 43rd Photovoltaic Specialists Conference (PVSC)*, 2016, pp. 2269–2273.

[20] R. J. Lovelett, G. M. Hanket, W. N. Shafarman, R. W. Birkmire, and B. A. Ogunnaike, "Design and experimental implementation of an effective control system for thin film Cu(InGa)$Se_2$ production via rapid thermal processing," *J. Process Control*, vol. 46, pp. 24–33, 2016.

[21] ICDD DDView 4.8.3.4 using PDF-2, "JCPDS - International Centre for Diffraction Data." Newtown Square, PA, 2008.

[22] W. K. Kim, "Study of Reaction Pathways and Kinetics in $CuIn_{1-x}Ga_xSe_2$ Thin Film Growth," University of Florida, 2006.

[23] S. Soltanmohammad, B. McCandless, and W. N. Shafarman, "A quaternary Laves-type phase in Ag-Cu-In-Ga thin films," *J. Alloys Compd.*, vol. 710, no. 2017, pp. 819–824, 2017.

[24] J. Weszka, P. Daniel, A. Burian, A. M. Burian, and A. T. Nguyen, "Raman scattering in $In_2Se_3$ and $InSe_2$ amorphous films," *J. Non. Cryst. Solids*, vol. 265, pp. 98–104, 2000.

[25] O. A. Balitskii, V. P. Savchyn, and V. O. Yukhymchuk, "Raman investigation of InSe and GaSe single-crystals oxidation," *Semicond. Sci. Technol.*, vol. 17, no. 2, pp. L1–L4, 2002.

[26] C. Julien, A. Khelfa, N. Benramdane, and J. P. Guesdon, "Preparation and characterization of $In_4Se_3$ films," vol. 27, pp. 53–60, 1994.

[27] C. Rincón and F. J. Ramírez, "Lattice vibrations of $CuInSe_2$ and $CuGaSe_2$ by Raman microspectrometry," *J. Appl. Phys.*, vol. 72, no. 9, p. 4321, 1992.

[28] E. P. Zaretskaya *et al.*, "Raman spectroscopy of $CuInSe_2$ thin films prepared by selenization," *J. Phys. Chem. Solids*, vol. 64, no. 9–10, pp. 1989–1993, 2003.

[29] C. Rincón *et al.*, "Raman spectra of the ordered vacancy compounds $CuIn_3Se_5$ and $CuGa_3Se_5$," *Appl. Phys. Lett.*, vol. 73, no. 4, pp. 441–443, 1998.

[30] H. W. King and T. B. Massalski, "Lattice spacing relationships and the electronic structure of H.C.P. ζ phases based on silver," *Philos. Mag.*, vol. 6, no. 65, pp. 669–682, 1961.

[31] J. H. Boyle, B. E. McCandless, W. N. Shafarman, and R. W. Birkmire, "Structural and optical properties of (Ag,Cu)(In,Ga)$Se_2$ polycrystalline thin film alloys," *J. Appl. Phys.*, vol. 115, no. 22, p. 223504, 2014.

[32] M. Grossberg, J. Krustok, I. Bodnar, S. Siebentritt, and J. Albert, "Photoluminescence and Raman spectra of the ordered vacancy compound $CuGa_5Se_8$," *Phys. B Condens. Matter*, vol. 403, no. 1, pp. 184–189, 2008.

[33] A. R. Jeong *et al.*, "Effects of substrates on structural and optical properties of Cu-poor $CuGaSe_2$ thin films prepared by in-situ co-evaporation," *Curr. Appl. Phys.*, vol. 13, no. 5, pp. 907–912, 2013.

[34] R. Krishnan *et al.*, "Reaction kinetics and pathways of $MoSe_2$," in *2010 35th IEEE Photovoltaic Specialists Conference*, 2010, pp. 001006–001008.

[35] J. H. Han *et al.*, "Actual partial pressure of Se vapor in a closed selenization system: quantitative estimation and impact on solution-processed chalcogenide thin-film solar cells," *J. Mater. Chem. A*, vol. 4, no. 17, pp. 6319–6331, 2016.